5th Canmet/ACI International Conference Durability of Concrete - Barcelona 4-9 June 2000 - Supplementary papers. Editor: V.M. Malhotra.

SIMULATION OF THE POROUS SYSTEM OF HYDRATING CEMENTITIOUS MATERIALS

P. Navi, C. Pignat and Y.F. Houst

Synopsis: Characterization of the pore structure of cementitious materials is of fundamental importance for the understanding of their mechanical and transport properties, and consequently for their durability.

Over the past ten years, computer models for simulating the hydrating and the microstructure forming of cement-based materials have been developed intensively. The models are of two types : “continuum-based models” and “digital image-based models”. An Integrated Particle Kinetics Model based on the continuum approach, for 3D simulation of the evolution of tricalcium silicate microstructure during hydration, is used in this study.

The evolution of the microstructure of hardened cement paste and the related development of strength and transport properties, depend strongly on the cement particle-size distribution. Using computer models to develop the microstructure of cement paste provides one with the possibilities for investigating the relation between particle-size distribution and microstructure, as well as properties. The pore-size distribution of simulated cement paste is determined by applying two different techniques: a 2D numerical Mercury Intrusion Porosimetry and a 3D Morphological Thinning and Partitioning of Void Space technique. The connectivity and the pore-size distribution of a hydrated cement paste have been calculated. The reliability of the techniques was also tested successfully in different ways.

Keywords: 3D simulation, Computer Modeling, Connectivity, Pore-size distribution, Porosity.

Parviz Navi, PhD, Privat-Docent, Member of RILEM TC 123 Committee "The Modeling of Microstructure and its Potentials for Studying Transport Properties and Durability", is active in research programs on micromechanics and rheology of concrete at the Laboratory for Building Materials, Swiss Federal Institute of Technology, Lausanne, Switzerland (EPFL).

Christian Pignat, materials science post graduate, research assistant, working on the modeling of the microstructure in cement-based materials during hydration at the Laboratory for Building Materials, Swiss Federal Institute of Technology, Lausanne, Switzerland (EPFL).

ACI member Yves F. Houst, a chemist, dr. ès sciences, is the Head of the *Cement Group* of the Laboratory for Powder Technology, Swiss Federal Institute of Technology, Lausanne, Switzerland (EPFL). He is involved in various research programs related to properties of cement suspensions, admixtures and durability of cementitious materials.

INTRODUCTION

The importance of the porosity of cementitious materials on their durability is well known, and will not be discussed here. Those who are interested in this subject should consult the specific literature, like for instance reference [1]. Hydrated cement paste (hcp) has a complex microstructure, varying in time and influenced by numerous parameters such as chemical composition, cement particle size distribution, W/C, temperature, etc. The construction of the complex microstructure of cement paste through 2D SEM images or from images obtained by X-ray computed microtomography, is extremely tedious and difficult. Mathematical or kinetic models can however simulate this microstructure. A comprehensive description of the different steps involved in the simulation of hydration and formation of structure of the hardened cement is given in [2].

The evolution of the microstructure of hardened cement paste and the related development of strength and transport properties, depend strongly on cement particle size distribution [3,4]. This dependency is particularly important for concrete at early age. Unfortunately, this dependency could not be studied due to difficulties existing on 3-D characterization of the microstructure of cement based materials. Using computer models to develop the microstructure of cement paste provides an excellent possibility for investigating the relationship between particle size distribution and related microstructure development. In reference [5], the computer model for simulating the hydrating and microstructure forming of cement-based materials Integrated Particle Kinetics (IPKM) was developed.

The aim of this work is to characterize the capillary pore structure of a simulated cement paste. After a brief introduction to the simulated microstructure, the following topics will be discussed: firstly, the validation by a 3D numerical technique recently developed and used for the determination of the pore-size distribution of simulated hydrated cement paste. This technique is called Morphological Thinning and Partitioning of the Void Space (MTPVS) [6]. Secondly, the application of two different techniques: a Mercury Intrusion Technique (MIT) and MTPVS to 2D images of simulated cement paste. The results obtained from these techniques will be discussed. It is worthwhile to note that the application of numerical MTPVS technique on a 2D or 3D pore space is

almost similar, but the use of numerical MIT on a 3D pore space is much more difficult than in 2D. Thirdly, pore-size distribution curves obtained through application of numerical MTPVS technique to 3D images of simulated hcp are given. Finally, some ideas about future work are reported.

MICROSTRUCTURE FORMATION

The particle-size distribution of anhydrous portland cement is currently in the range 1 - 50 µm. After mixing with water, portland cement hydrates and new phases appear: calcium hydroxide (CH) and hydrated calcium sulfoaluminates crystals, and C-S-H particles of colloidal dimensions. The anhydrous phases disappear as a consequence of the formation of hydrated phases. The pore-size distribution of such system becomes very wide. The C-S-H is composed of irregular layers that create interlayer spaces in the range 0.5 - 2.5 nm. According to IUPAC [7], these pores are essentially micropores (< 2 nm). The two other solid phases are composed of large crystals of calcium hydroxide (portlandite) and hydrated calcium sulfoaluminates (monosulfate and ettringite) in the µm range. The original space between anhydrous cement particles is not completely filled by hydration products and the size of capillary voids range from 10 nm to 1 µm. But, in well hydrated, low water/cement pastes, these voids are smaller than 100 nm [8]. Furthermore, hcp contains voids due to entrained air (50 µm - 1 mm) and entrapped air voids (1 - 5 mm). As a conclusion, pores in hcp range from 0.5 nm to 5 mm, that means 7 orders of magnitude. The situation is not very different in concrete, since it can only have some larger air voids and defects due to uncompleted compaction of the fresh mixture.

MORPHOLOGICAL THINNING AND PARTITIONING VOID SPACE (MTPVS)

Description of MTPVS

This numerical approach is a variant of the morphological thinning method. A general explanation of this approach is given in reference [9]. This can be applied to a pore space demonstrated by images to partition the void space into a well-defined collection of individual pores. Each individual pore consists of a site bounded with interfaces with solid matrix, and by pore necks. A pore neck is defined as a plane where the hydraulic radius (area divided by its perimeter) has a local minimum. From the segmented pores several useful data such as pore-size distribution curve and surface to perimeter ratio can be obtained. By using this approach, the effects of cement particle distribution on pore size distribution of 3D simulated microstructure of hcp have been investigated [10].

Prior to this approach, the pore structure had to be represented by regular pixels (or voxels for 3D images). Each pixel will then represent either a solid or a pore part. Because of the wide range of the pore sizes in hcp, it is evident that the size of the pixel has a strong influence on its pixel representation as well as on the pore-size distribution. Using pixels having a very small size, one can obtain an accurate pore-size distribution. Let us consider that at time t the 3D microstructure is simulated and is prepared for evaluating its pore-size distribution with a pixel size d, so the computational volume is given by $a^3 = (n \times d)^3$, where n is an integer.

The MTPVS technique consists of three stages: thinning, rebuilding, and computing equivalent radius of the individual pores. The thinning can be applied to an image when pixels or voxels represent it. The aim of this operation is to replace the pore space with layers of pore pixels. The result of such thinning algorithm in a 2D image is shown in Fig. 1. During the morphological thinning, the pore pixels are removed from the surface of the pore space, layer by layer inwards giving each layer a number starting with one. This part of operation is called pore erosion or solid dilation.

When all the porous pixels are eroded, the second stage starts by rebuilding the pore space, layer by layer outward, beginning with the last eroded layer. This operation partitions the pore space into a set of individual pores. A discrete layer having a local maximum layer number (stomach) and a set of necks separating the pores identify each individual pore. The necks and stomachs are defined as shown in Fig. 2, which illustrates an example of two distinct pores in two dimensions. Application of MTPVS technique is basically the same for both two and three dimensions. In Fig. 2, the stomach of pore 1 is made by two pixels (layer 4) which is discrete and has local maximum layer number. The stomach of pore 2 is built of five pixels (layer 3) which is discrete and possesses local maximum layer number. Layer 2 does not represent any stomach. The neck pixels between the two pores 1 and 2 are defined according to their equal distance with reference pixels of the pores. Reference pixels are the nearest pixels of the layer with smallest layer number, which separate the two pores. The line indicates the neck defined with respect to the two reference pixels of pores 1 and 2 in Fig. 2.

All statistics related to the characterization of pore space such as pore size distribution, volume to surface ratio, etc. can readily be determined by this technique. For each single pore its volume and surface are determined, then corresponding equivalent shape radius was estimated. It should be noted that there is no common accepted definition for equivalent shape radius. For the purpose of validation the MTPVS technique two 3D examples have been examined. In these examples, the pores were considered spherical and the radius was determined from the corresponding volume. Beside, the hydraulic radius for each pore has been calculated.

Inversion of the solid and the pores in a granular-porous structure

Let us mix spherical particles with a known particle-size distribution with water. A 2D cut of this mixture with periodic boundary conditions is represented in Fig. 3A. The computational volume considered is 100 x 100 x 100 μm^3, and the W/C 0.4. The number of particles is 196. Then, this mixture has been inverted by changing the place of the water and the particles to get Fig. 3B. In this figure the black represents the solid and the white the spherical pores. The pore-size distribution of Fig. 3B is the same as the particle-size distribution of Fig. 3A given in Fig. 4.

MTPVS technique has been applied to the 3D structure shown in Fig. 3B with a voxel dimension of 0.5 μm. The pore-size distribution obtained from the numerical application corresponds exactly to the particle-size distribution of Fig. 3A.. The pore effective radius is calculated from the pore volume. The second curve given in Fig. 4, was obtained by dividing the pore volume by its surface. This curve gives finer pores when compared to the exact one. This discrepancy is due to the fact that in the numerical calculation, the structure is replaced by

the 3D voxels. This change transfers the pore surface to a bigger surface compared to the exact one.

Hexagonal primitive packing of spheres

For a second example, numerical results were compared to experimental ones given in reference [11], where Nitrogen adsorption and mercury porosimetry were used for analyzing the pore structure of close-packed silica spheres. This packing has a unique array formed of the same layers stacked vertically one above the other. Figs. 5 and 6 show this closest packing within a layer and in space lattice respectively. The rectangle in Fig. 5 represents the base of the space lattice. In this packing one silica sphere has a diameter of 310 nm.

To apply MTPVS technique to this 3D porous structure, a computational volume of 2170 x 2170 x 2170 nm^3 was chosen. This volume consists of 392 spheres and 784 similar pores. In this structure, the basic rectangle shown in Fig. 5 was slightly changed, to 1.75 x 1 the sphere diameter, instead of 1,73. This was made to keep the computational volume a cubic one with periodic boundary condition. The resulting periodic structure is shown in Fig. 7, with a 2D cut in passing through the middle of spheres.

Fig. 8 shows the cumulative pore-size curve of the structure, calculated by MTPVS technique. The size of the voxel used in this example was 9.69 nm with total of 224 x 224 x 224 voxels. Results show a unique pore shape with hydraulic radius equal to 52.3 nm. A small discrepancy shown in the Fig. 8 is due to the precision of coordinates of the grain or due to the algorithm used. The total porosity was calculated by summing up the pore volumes, which gives a porosity of 39.5 %, the same as shown in [11]. The BET specific surface area was also determined and the results are given in the same paper. A value of 14,2 m^2/g was found. The corresponding calculated result by MTPVS technique is 25.7 m^2/g. As we discussed in the first example, this difference may be due to the fact that in the MTPVS technique a real structure is replaced by voxels, and the pore surfaces are changed to planes oriented in three directions. Then the calculated surface depends strongly to the voxel size. If pores are considered spherical, the calculated equivalent pore radius becomes 107.4 nm, which is two times bigger than the mean hydraulic radius. The difference between these values (a factor 2) shows that the pore shape is different from a sphere. This difference can however provide a factor of pore shape. More these values are similar, more the pore shape is spherical.

APPLICATION OF MIT AND MTPVS TECHNIQUES TO 2D IMAGES

Numerical mercury porosimetry technique

In mercury intrusion, according to Laplace-Young equation, the pressure is proportional to the curvature of the mercury meniscus. For a cylindrical pore, a unique radius defines the corresponding curvature. For a non-cylindrical pore, the corresponding curvature is a combination of two radii. This makes the

numerical application of mercury intrusion technique to a simulated 3D pore space very difficult. Therefore, this technique was applied to a 2D porous structure where the menisci are circular and the contact angle between solid and mercury is considered to be 180°.

The numerical application of mercury intrusion technique to 2D images follows a procedure similar to experiment. It starts from the edges of the 2D image, filling the accessible pores with circles of a given diameter. This process of filling is carried out by reducing the diameter and is repeated until the pore space is filled out completely, as it shown in Fig. 9.

For each diameter the corresponding occupied surface is calculated. By varying the diameter, a complete intrusion curve can be produced for the considered microstructure. The result of such a numerical approach on a 2D slice of simulated hydrated C_3S is given in Fig. 9. In this example blocks represented in black are solids and the meniscus diameter varies with gray level from 5 to 0.5 mm.

The corresponding pore-size distribution curves computed for three different slices at 50, 75 and 100 micrometers distance from the boundary of computational volume are given in Fig. 10. Garboczi and Bentz [12] have obtained, for a 2D microstructure, the pore-size distribution using the same technique, but applied to digital images.

Pore-size distribution curve using the MTPVS approach

Three 2D images identical to those studied with the numerical Mercury Intrusion Technique were selected for application of the MTPVS approach. The result corresponding to Fig. 1 is given in Fig. 11, each individual pore as defined before is shown by a different gray level.

Based on the definition given for the equivalent pore radius, the radius of each individual pore has been calculated, as well as its volume and surface. The cumulative pore-size curves of three 2D slices have been computed and the corresponding results are given in Fig. 12.

3D characterization of the pore space of a simulated hydrated cement paste by use of the MTPVS

How to apply the numerical mercury intrusion technique to a three dimensional pore structure to obtain the pore size distribution is not obvious. On the contrary, as we have explained before, MTPVS can be applied readily to three and two dimensional images almost in the same manner. This method was applied for calculating the pore-size distribution curve of the simulated C_3S paste at different hydration times. As an example, a 80 X 80 X 80 μm^3 computational volume was considered. The C_3S grains were spherical and possessed a particle size distribution varying from 2 mm to 30 mm. The W/C was 0.4 and the number of grains was 1919. The pore space was represented by voxels of 0.5 mm on a side. The cumulative pore-size curves of the pore spaces at different hydration times were calculated and are shown in Fig. 13.

The connectivity of the pore spaces at different hydration steps was also computed by using an algorithm proposed in reference [13]. This algorithm bears on three-dimensional representation of a microstructure with successive two-dimensional slices. The connectivity of pores can be evaluated with precision by using voxels of a very small size [5]. The connectivity of the pore spaces represented with voxels of 0.5 μm on a side and the porosity at different hydration times are given in Fig. 14.

Illustrating the three dimensional image of partitioned pore space is difficult. Two-dimensional sections of the partitioned pore space of three-dimensional numerical hydrated C_3S paste at different stages of hydration are given in Figs. 15 to 17. These figures show the evolution of individual pores and the solid parts (solid parts consist of C_3S and hydrated parts: C-S-H and CH) in a period of one week represented by 2D cuts. The black indicates the solid, to each partitioned pore a gray level is attributed.

DISCUSSION AND CONCLUSION

The pore-size distribution of the pores in the range 5 μm - 0.5 μm radius has been computed, from 2D and 3D images of simulated hydrated C_3S paste. Two different techniques have been developed namely: a Mercury Intrusion Technique (MIT) and a Morphological Thinning and Partitioning of Void Space (MTPVS). Numerical application of MIT to simulated 3D pore space is difficult, while MTPVS can be applied to 3D images. The accuracy of this numerical method by using two 3D examples has been tested. The method has been applied successfully to 3D images and gives accurate results. Nevertheless, the calculated pore surface is always higher than the real one. This is due to the fact that prior to application the MTPVS to 3d images the real structure had to be replaced by voxels. The first results show that this increase in the surface can reach about 50%.

Numerical MIT and MTPVS were applied separately to 3 slices obtained from 3D simulated hydrated paste. Figs. 10 and 12 show the cumulative pore-size curves obtained from MIT and MTPVS respectively. Comparing the results given in Fig. 10 with those in Fig. 12 indicates strong discrepancies between curves belonging to the same images. MTPVS has been applied to 2D images to obtain an accurate pore-size distribution for comparison with results obtained by MIT. It should be noted that in MTPVS technique, the shape of the cumulative pore-size curve depends on the definition of equivalent pore radius. In spite of that, the curves shown in Fig. 12 should present a reasonably accurate cumulative pore-size of pores between 5 μm and 0.5 μm. Because the pore space of cement paste is complex and composed of interconnected non-cylindrical discrete pores, the derivation of pore size distribution from MIT by using simple model can give misleading results. Fig. 12 shows a much less percentage of small pores than suggested by mercury intrusion test.

MTPVS has been applied to 3D images. Two dimension images of partitioned pore space are illustrated in Figs. 15 to 17. To each pore a gray level is

attributed to differentiate from other pores at each hydration time. The evolution of C_3S paste microstructure, specially the nucleation of CH in water, changes the shape and the pore-size distribution. This variation can be observed in Figs. 15 to 17. The computed pore-size distribution curves for C_3S at different hydration times are given in Fig. 13. The curves show that, during hydration, the porosity and the mean hydraulic radius decrease. There is no difference between results for hydraulic radii of 0.3 and 0.6 μm, because the pixel dimension was 0.5 μm. Fig. 14 shows that the connectivity of the pore space only falls down for hydrated C_3S with porosity less than 10%. It is important to note that this result depends strongly on the pixel dimension. For smaller pixel dimension, the result would be more accurate and it is possible that this connectivity stays equal to one (almost all pores remaining connected even for the last hydration steps).

The comparison between the results obtained on 3D images using two different techniques may permit to calibrate the experimental results obtained by MIT. There is not a clear understanding of the description of the pore space of the cement-based materials. The results from characterizing the pores of simulated hydrated C_3S indicate that in a paste with less than 10% porosity, almost 95% of capillary pores smaller than 2 μm diameter are connected [5].

Recently, models have been developed for simulating the cement hydration microstructure and numerical tools for computing the porosity, connectivity of pores, hydraulic radius as well as three-dimension pore-size distribution of simulated cement paste. The cement hydration with real particle-size distribution varying between 3 μm to 40 μm has been simulated. Its pore space covering two orders of magnitude has also been characterized. Porosity of cement-based materials covers several orders of magnitude, ranging from nanometers to millimeter. A realistic microstructure model should describe the pores at several scales. The major challenge is now to develop multiscale model to describe quantitatively the microstructure of cementitious materials.

ACKNOWLEDGMENTS

Financial support from the Research Foundation of the Swiss Cement Industry (VSZKGF) and Swiss Office for Education and Science (OFES) is gratefully acknowledged.

REFERENCES

1 Kropp, J. and Hilsddorf, H.K. (Editors), Performance Criteria for the Concrete Durability, E & FN Spon, London, etc., 1995.

2 Van Breugel, K., Simulation of hydration and formation of structure in hardening cement-based materials, Thesis, Delft Technical University, Delft, The Netherlands, 1991.

3 Granju, J. L. and Maso, J. C., Hardened Portland cement pastes, modelisation of the microstructure and evolution laws of mechanical properties. I- Basic results, II- Compressive strength law, Cement and Concrete Research, Vol. 14,, pp. 249-256, 1984.

4 Quenard, D., Xu A., Künzel, K., Hartwig, M. Bentz, D.P. and Martys, N.S., Microstructure and transport properties of porous building materials, Materials and Structures, Vol. 31, pp. 317-324, 1998.

5 Navi, P., Pignat, C., Simulation of cement hydration and the connectivity of the capillary pore space, Advanced Cement Based Materials, Vol. 4, pp. 58-67, 1996.

6 Navi, P. and Pignat, C., 3D characterization of the pore structure of a simulated cement paste, Cement and Concrete Research, vol. 29, pp. 507-514, 1999.

7 IUPAC, Reporting Physisorption Data for Gas/Solid Systems with Special Reference to the Determination of Surface Area and Porosity, Pure & Applied Chemistry, Vol. 67, No 4, pp. 603-619, 1985.

8 Mehta, P.K., Concrete: Structure, Properties and Materials, Prentice-Hall INC., Englewood Cliffs, NJ, USA, pp. 23-27, 1986.

9 Baldwin C. A., Sederman, A. J., Mantle, M. D, Alexander, P. and Gladden, L.F, Journal of Colloid and Interface Science, Vol. 181, pp. 79-99, 1996.

10 Navi, P. and Pignat, C., Effects of cement size distribution on capillary pore structure of the simulated cement paste, Journal of Computational Materials Science, vol. 16, pp. 285-293, 1999.

11 Bukowiecki, S., Straube, B. and Unger, K.K., Pore structure analysis of close packed silica spheres by means of nitrogen sorption and mercury porosimetry, Principles and applications of pore structural characterization (Haynes, J.M. and Rossi-Doria, P., Eds), J.M. Arrowsmith LTD, Bristol, G.B., pp. 43-55, 1985.

12 Garboczi, E.J.and Bentz, D.P., Advances in Cementitious Materials, Ceramic Transactions, Vol. 16, pp. 365-380, 1991.

13 Hoshen,J., Kopelman R., Physical Review. B, Vol. 14, pp. 3438-3445, 1976.

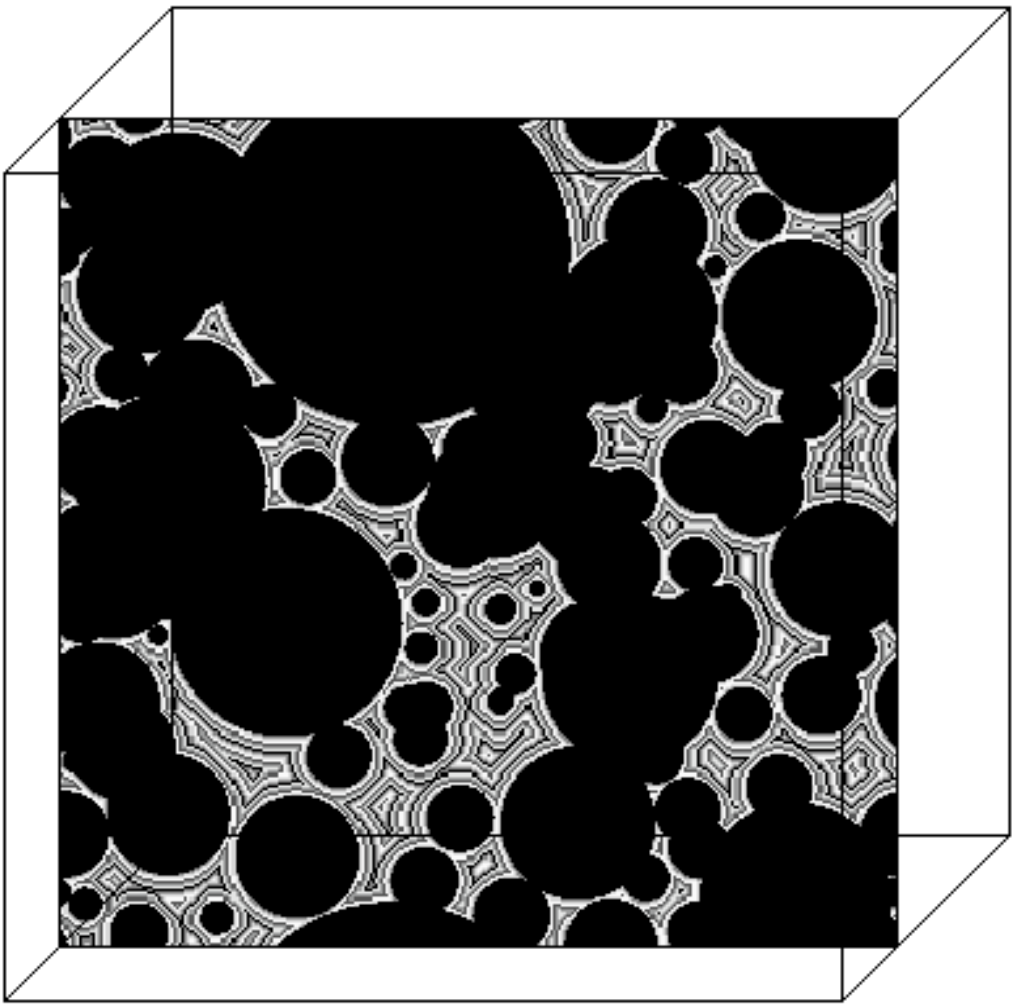

Fig. 1: Thinning of two-dimensional image of pore space.

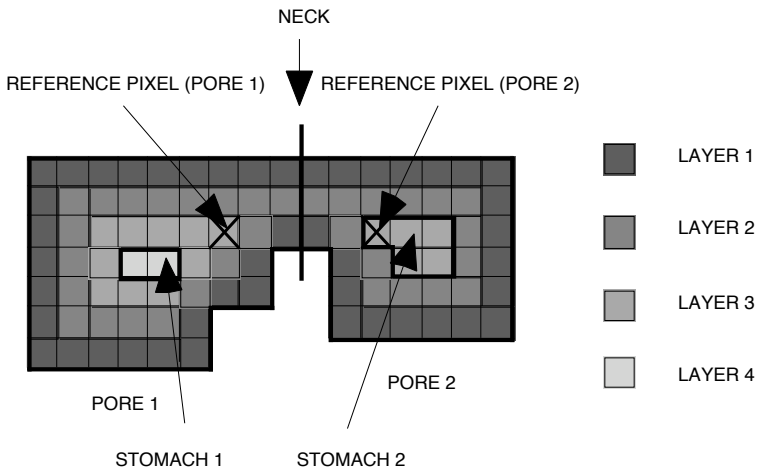

Fig. 2: Partitioning of the pore space into pore 1 and pore 2.

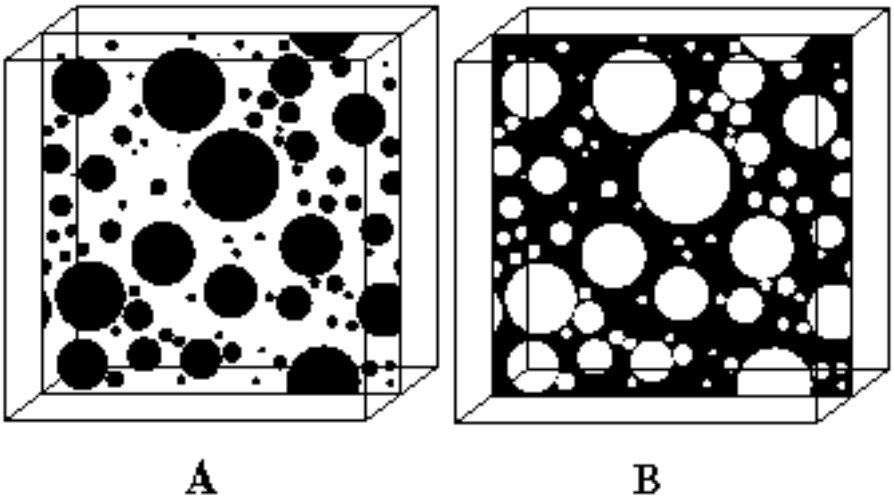

Fig. 3 (A) Representation a 2D slice cut from 3D water-spherical particle mixture and (B) inverted of (A), represents a 2D slice cut from 3D solid spherical pores.

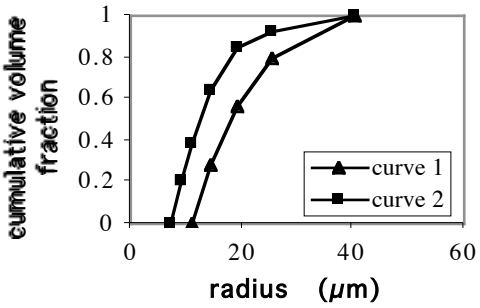

Fig. 4: Curve 1 represents cumulative particle-size used in Fig. 3 (A) in water particle mixture and calculated pore-size of Fig. 3 (B) by MTPVS technique. Curve 2 represents calculated cumulative hydraulic radii of pores in Fig. 3 (B).

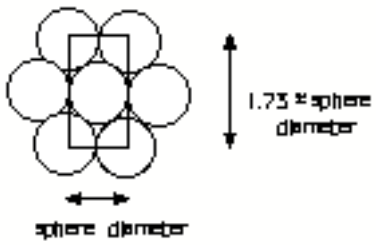

Fig. 5: Representation of seven closed-packed silica spheres within a layer.

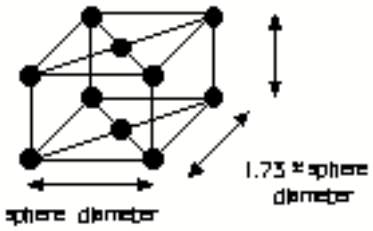

Fig. 6: Schematic representation of silica spheres cube within two layers.

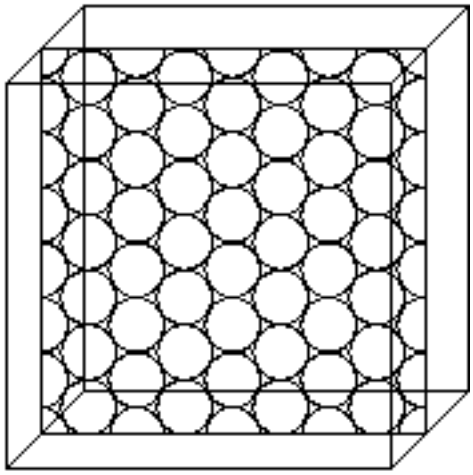

Fig. 7: Schematic representation of computational volume, 2170 * 2170 2170 nm^3 with periodic boundary conditions, consisting of pores and spherical particles. A 2D slice is cut through the middle of spheres

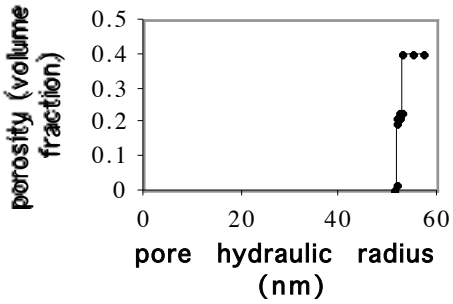

Fig. 8: Cumulative pore-size curve of closed-packed silica spheres pore structure.

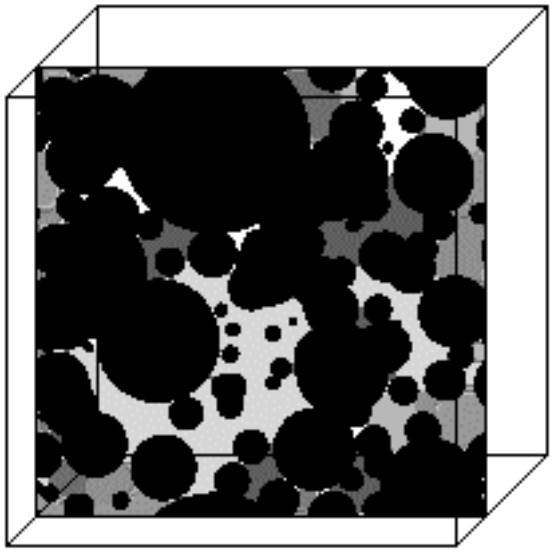

Fig. 9: Final penetration of mercury shown by different gray levels, each corresponding to minimum meniscus diameter for mercury penetration. The white indicates the pores not penetrated by the minimum meniscus diameter of 0.5 μm.

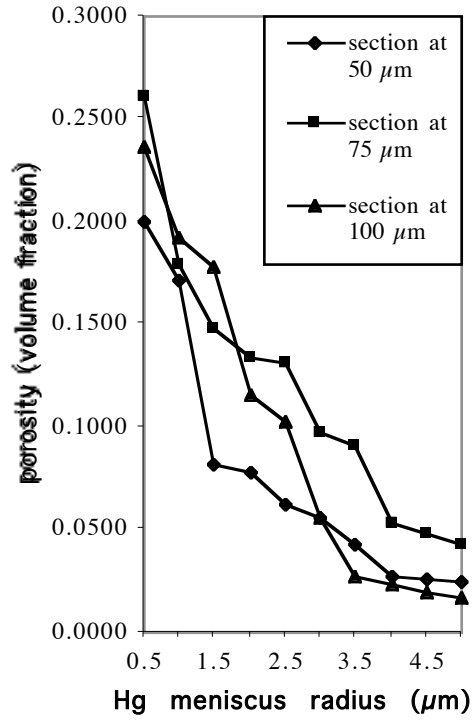

Fig. 10: Cumulative pore size distribution curves determined from using the numerical Mercury Porosimetry Technique on the 2D image.

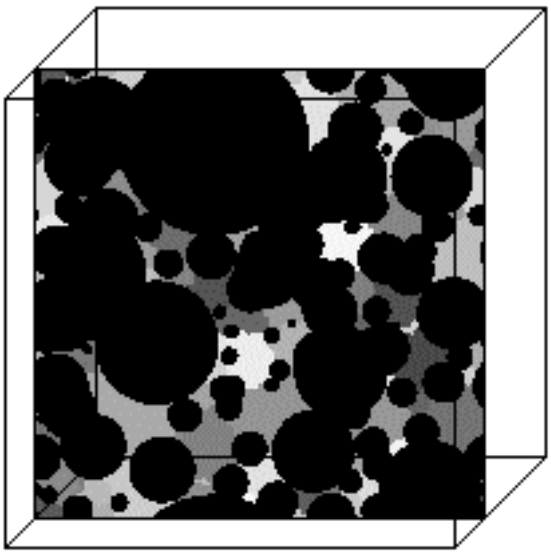

Fig. 11: The partitioning of the pore space of a 2D simulated cement pore. Each gray level shows an individual pore and the black indicates the solid.

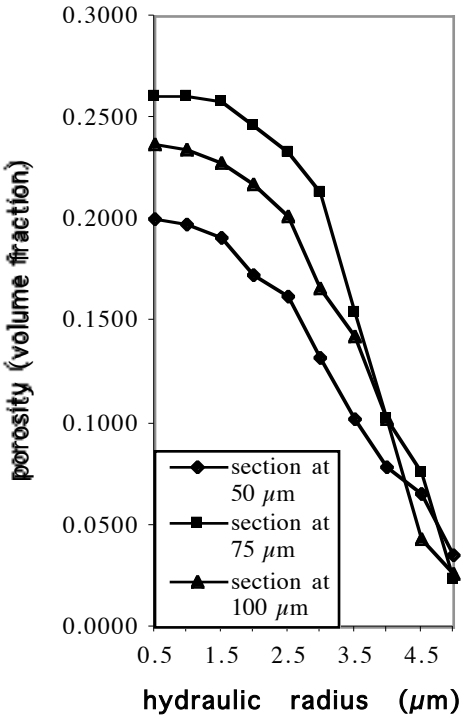

Fig. 12: Cumulative pore size curves obtained for 3 sections at 50, 75 and 100 micrometers distance from the boundary of computational volume, using the MTPVS.

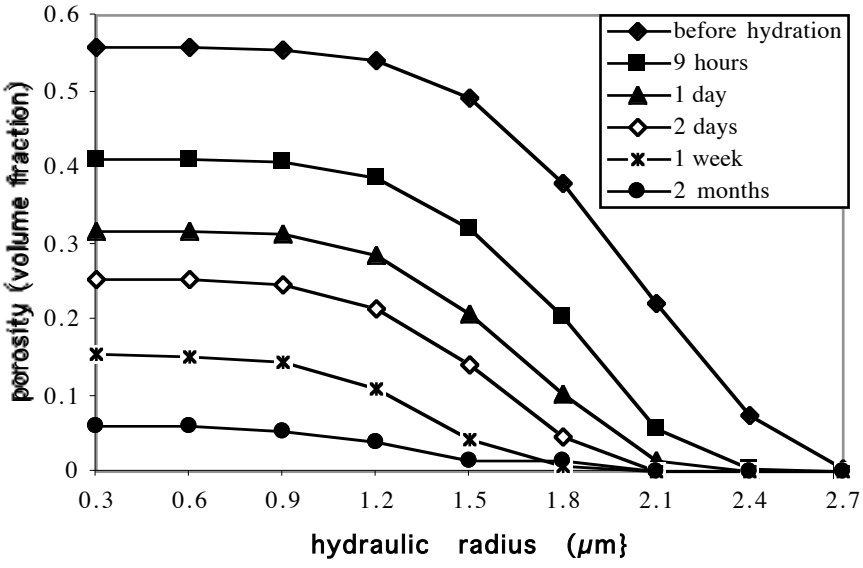

Fig. 13: Cumulative pore-size curves for a three-dimensional specimen according to the MTPVS technique and at different hydration times.

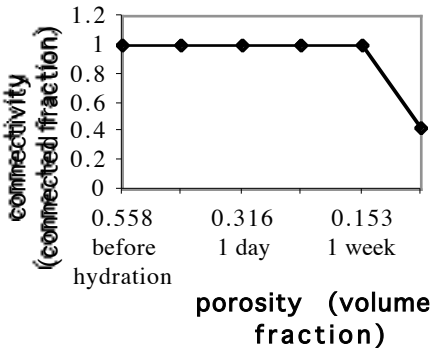

Fig. 14: connectivity of the porosity for the different hydration times.

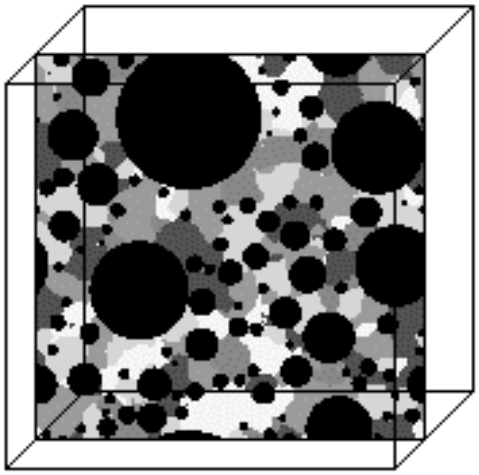

Fig. 15: 2D section in the middle of the specimen before hydration, the black indicates the solid.

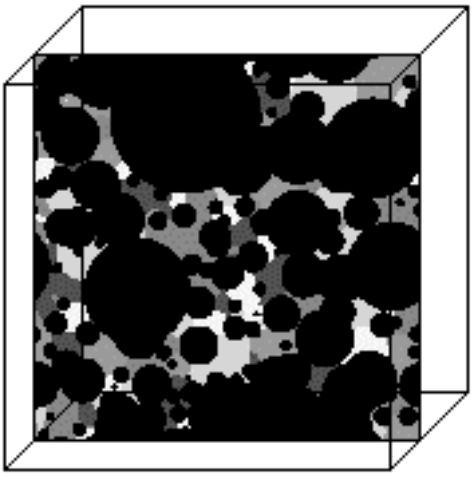

Fig. 16: 2D section in the middle of the specimen after one day hydration.

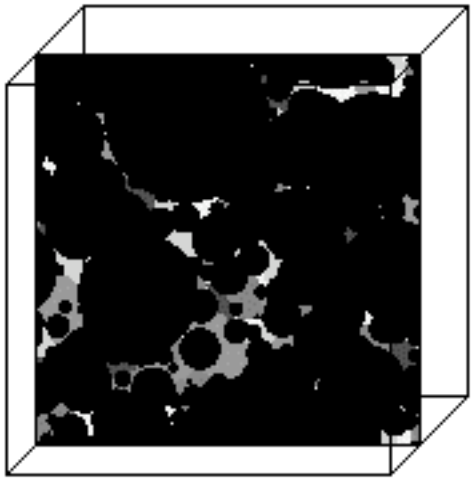

Fig. 17: 2D section in the middle of the specimen after one week hydration.